

Diboson productions and aTGCs search at LHC

Yusheng Wu^{1,2,a}, on behalf of ATLAS and CMS collaborations

¹University of Michigan

²University of Science and Technology of China

Abstract. The ATLAS and CMS collaborations have measured the production cross-sections of dibosons (WW , WZ , ZZ , $W\gamma$, $Z\gamma$) in leptonic decay final states with collision data produced at the LHC with both $\sqrt{s} = 7$ TeV and $\sqrt{s} = 8$ TeV. Based on these data, limits on anomalous triple-gauge-couplings are also derived.

1 Introduction

The Standard Model (SM) electroweak theory is based on the $SU(2)_L \otimes U(1)_Y$ gauge groups, in which the gauge symmetry is spontaneously broken by the Higgs mechanism. The studies of diboson productions at LHC help to test the theory at TeV scale, improve the understanding of background processes in Higgs searches and also offer great opportunities to search for new physics at the high energy frontier.

At leading order, dibosons are produced mainly through $q\bar{q}$ annihilation, while gg fusion contributes typically less than 10% [3]. The diboson productions of WW , WZ , ZZ and $W/Z + \gamma$ are studied in leptonic decay final states. Diboson production cross-sections are known to next-to-leading order (NLO) in QCD, and the electroweak radiation corrections to the cross-sections are important at high \sqrt{s} [4]; besides, the leptonic decay final states offer clean signature and enable the possibility of precision measurements. These cross-section measurements therefore provide crucial and sensitive test of both QCD and electroweak theory at the TeV scale.

Many new physics models predict resonance particles that can decay to boson pairs. Some of these models are based on the non-SM implementation of electroweak symmetry breaking; for instance, there are little Higgs [5], technicolor [6], extended gauge models [7] and Randall-Sundrum graviton [8] models. These new particles can be searched in either fully leptonic or semileptonic decay final states of diboson events, and the high energy of the LHC offers the greatest potential. A direct search for new resonances is not covered in this paper, instead an indirect approach is carried out by searching for anomalous triple-gauge-couplings (aTGCs). In the SM, triple-gauge-couplings (TGCs) are completely determined by gauge theory; and any deviation from the SM couplings indicates existence of new physics beyond the SM. aTGCs depend strongly on the center of mass energy of the colliding

bosons; therefore, the LHC offers a great opportunity for measuring stringent limits. Besides, aTGCs largely manifest themselves in high momentum or high mass regions, the sensitivity can be further enlarged by proper binning of kinematics distributions.

The reported analysis results are based on the pp collision data collected by the ATLAS [1] and CMS detectors [2] during the years of 2011 and 2012. The integrated luminosities of analyzed data are slightly different among various diboson channels; but the maximum amount of data in use corresponds to about 5 fb^{-1} at both $\sqrt{s} = 7$ TeV and $\sqrt{s} = 8$ TeV. The detectors were operating amazingly well during the data taking periods; the detectors operated at a fraction of above 95% operational channels and data taking efficiencies were higher than 93%. The following sections will describe both the results of cross-section measurements and aTGCs search.

2 Cross-section measurement

2.1 Overview

As an overview, Figure 1 shows the measured production cross-sections of various diboson processes and their comparisons with SM NLO predictions from the ATLAS and CMS experiments [9, 10]. The measurements are consistent with theoretical predictions.

2.2 $W/Z + \gamma$

In this channel, events with a leptonic decay boson (W or Z) and a photon are selected. Major background processes include $W/Z + jets$ and $\gamma + jets$, where jet-induced photons or jet-faking leptons are selected. In order to suppress these backgrounds, events with low boson mass or low E_T^{miss} are rejected, and in addition photons are required to be separated from leptons. The total systematic uncertainty for the measured cross-section is about 7 – 9%; the major ones come from photon reconstruction and the background estimation. The cross-sections are measured

^ae-mail: Yusheng.Wu@cern.ch

in bins of the transverse photon energy (E_T^γ), and presented in Figure 2 [11, 12].

2.3 WW

WW events are selected to have two high p_T isolated leptons and large E_T^{miss} . Backgrounds consist of $t\bar{t}$, $Z + jets$, $W + jets$ and other diboson processes. The signal is purified by removing events within Z mass windows, rejecting events with one or more jets and discarding low $p_T^{\ell\ell}$ (transverse momentum of two lepton system) region. The dominant source of uncertainty is the jet-veto uncertainty, and the total systematic uncertainty is around 8%. Measured cross-sections are in agreement with theory, which are presented in Table 1 [13, 14].

2.4 WZ

Three leptons plus large E_T^{miss} make this signature very clean, but there are still background events contributing from ZZ, $Z + jets$ and $t\bar{t}$. An on-shell Z and a W boson with large transverse mass are required in these events in order to further suppress the contamination. The systematic uncertainties mainly come from lepton and E_T^{miss} reconstructions, which turns out to be around 5%. The measured cross-sections are shown in Table 2 [15, 16].

2.5 WW/WZ $\rightarrow \ell\nu jj$

In this analysis, the semi-leptonic decays of diboson are studied. The signal events have one lepton, large E_T^{miss} and two separated jets, where the jets are from hadronic W or Z boson decay. The irreducible $W + jets$ background is subtract using template fit method, and the combined cross-section of WW + WZ is derived as shown in Table 3 [17, 18], where the large systematic uncertainty is driven by uncertainties in the background estimation.

2.6 ZZ

The ZZ production cross-section is measured in two decay modes: $ZZ \rightarrow 4\ell$ and $ZZ \rightarrow \ell\ell\nu\nu$. In the four lepton case, the signature is very clean with background contribution of less than 2% after requiring two on-shell Z bosons for the signal selection. The measured cross-sections in both ATLAS and CMS are shown in Table 4 [19, 20]. In the two lepton plus E_T^{miss} channel, there is large background contamination from $Z + jets$, $t\bar{t}$ and other diboson processes. Apart from selecting an on-shell Z, events are further required to have zero jets, large E_T^{miss} in the Z transverse momentum direction. The measured cross-section in ATLAS at $\sqrt{s} = 7$ TeV is $5.4_{-1.2}^{+1.3}(\text{stats.})_{-1.0}^{+1.4}(\text{syst.}) \pm 0.2(\text{lumi.})$ pb [21], which is consistent with SM NLO prediction.

3 aTGCs search

The search is generally based on kinematics distribution of the boson p_T or the mass of the diboson system. Then

likelihood functions are constructed and systematic uncertainties are incorporated as nuisance parameters. The 95% confidence interval (CI) of aTGCs parameters are derived using statistics tools, such as $\Delta\log$ -likelihood, Bayesian or Frequentist methods. Results are presented in the following: Figure 3 shows the CI derived for aTGCs parameters in WWZ and WW γ vertices through WW, WZ and W γ production [11, 13, 15]. Figure 4 shows the limits for aTGCs parameters in ZZZ and ZZ γ vertices through ZZ production [20, 22]. Figure 5 shows the limits for aTGCs parameters in ZZ γ and Z $\gamma\gamma$ vertices through Z γ production [11, 12]. Results show consistency with SM couplings, therefore no anomaly is observed. The limits for aTGCs derived here are more stringent than those derived at the Tevatron, and in certain channels these are better than those from LEP.

4 Summary

Thanks to the very successful running of LHC and smooth operations of the ATLAS and CMS detectors, the diboson production cross-sections are measured in many channels and found to be consistent with the SM predictions. Data agree with SM couplings in aTGCs searches, and the derived 95% CI limits are improving existing results from Tevatron and are comparable with those from LEP.

References

- [1] ATLAS Collaboration, JINST **3**, S08003 (2008)
- [2] CMS Collaboration, JINST **3**, S08004 (2008)
- [3] John M. Campbell etc., JHEP **07**, 018 (2011)
- [4] Mark S. Neubauer, Annu.Rev.Nucl.Part.Sci. **61**, 223-250 (2011)
- [5] Perelstein M.Prog., Part.Nucl.Phys. **58**, 247 (2007)
- [6] Lane K., Phys.Rev.D **60**, 075007 (1999)
- [7] Pati JC etc., Phys.Rev.D **10**, 275 (1974)
- [8] Randall L. and Sundrum R., Phys.Rev.Lett. **83**, 3370 (1999)
- [9] <https://twiki.cern.ch/twiki/bin/view/AtlasPublic/CombinedSummaryPlots>
- [10] <https://twiki.cern.ch/twiki/bin/view/CMSPublic/PhysicsResultsEWK>
- [11] ATLAS collaboration, Phys.Lett.B **717**, 49 (2012)
- [12] <https://twiki.cern.ch/twiki/bin/view/CMSPublic/PhysicsResultsEWK11009>
- [13] ATLAS collaboration, Phys.Lett.B **712**, 289-308 (2012)
- [14] CMS-PAS-SMP-12-005,CMS-PAS-SMP-12-013
- [15] CERN-PH-EP-2012-179
- [16] CMS-PAS-EWK-11-010
- [17] ATLAS-CONF-2012-157
- [18] CMS collaboration, CERN-PH-EP-2012-311
- [19] ATLAS-CONF-2012-026,ATLAS-CONF-2012-090
- [20] CMS collaboration, CERN-PH-EP-2012-336, CMS-PAS-SMP-12-014
- [21] ATLAS-CONF-2012-027
- [22] CERN-PH-EP-2012-318

Table 1. The measured WW cross-sections in ATLAS and CMS (referenced from Table 6 of [13] and Section 7 of [14]).

Experiment	\sqrt{s}	$\int L(\text{fb}^{-1})$	$\sigma(pp \rightarrow WW)(\text{pb})$	SM NLO prediction (pb)
ATLAS	7TeV	4.6	$51.9 \pm 2.0(\text{stats.}) \pm 3.9(\text{syst.}) \pm 2.0(\text{lumi.})$	$44.7^{+2.1}_{-1.9}$
CMS	7TeV	4.9	$52.5 \pm 2.0(\text{stats.}) \pm 4.5(\text{syst.}) \pm 1.2(\text{lumi.})$	-
CMS	8TeV	3.5	$69.9 \pm 2.8(\text{stats.}) \pm 5.6(\text{syst.}) \pm 3.1(\text{lumi.})$	$57.3^{+2.4}_{-1.6}$

Table 2. The measured WZ cross-sections in ATLAS and CMS (referenced from Section 6.1 of [15] and Section 5.4 of [16]).

Experiment	\sqrt{s}	$\int L(\text{fb}^{-1})$	$\sigma(pp \rightarrow WZ)(\text{pb})$	SM NLO prediction (pb)
ATLAS	7TeV	4.6	$19.0^{+1.4}_{-1.3}(\text{stats.}) \pm 0.9(\text{syst.}) \pm 0.4(\text{lumi.})$	$17.6^{+1.1}_{-1.0}$
CMS	7TeV	1.1	$17.0 \pm 2.4(\text{stats.}) \pm 1.1(\text{syst.}) \pm 1.0(\text{lumi.})$	-

Table 3. The measured $WW + WZ$ cross-sections in ATLAS and CMS through semi-leptonic decay channels (referenced from Section 7 of [17] and Page 5 of [18]).

Experiment	\sqrt{s}	$\int L(\text{fb}^{-1})$	$\sigma(pp \rightarrow WW + WZ)(\text{pb})$	SM NLO prediction (pb)
ATLAS	7TeV	4.6	$72 \pm 9(\text{stats.}) \pm 15(\text{syst.}) \pm 13(\text{MC stats.})$	63.4 ± 2.6
CMS	7TeV	5.0	$68.9 \pm 8.7(\text{stats.}) \pm 9.7(\text{syst.}) \pm 1.5(\text{lumi.})$	-

Table 4. The measured ZZ cross-sections in ATLAS and CMS through fully leptonic decay channels (referenced from Section 6 of [19] and Section 7 of [20]).

Experiment	\sqrt{s}	$\int L(\text{fb}^{-1})$	$\sigma(pp \rightarrow ZZ)(\text{pb})$	SM NLO prediction (pb)
ATLAS	7TeV	4.6	$7.2^{+1.1}_{-0.9}(\text{stat.})^{+0.4}_{-0.3}(\text{syst.}) \pm 0.3(\text{lumi})$	$6.5^{+0.3}_{-0.2}$
CMS	7TeV	5.0	$6.2^{+0.9}_{-0.8}(\text{stat.})^{+0.4}_{-0.3}(\text{syst.}) \pm 0.1(\text{lumi})$	-
ATLAS	8TeV	5.8	$9.3^{+1.0}_{-1.1}(\text{stat.})^{+0.4}_{-0.3}(\text{syst.}) \pm 0.3(\text{lumi})$	7.4 ± 0.4
CMS	8TeV	5.3	$8.4 \pm 1.0(\text{stats.}) \pm 0.7(\text{syst.}) \pm 0.4(\text{lumi.})$	-

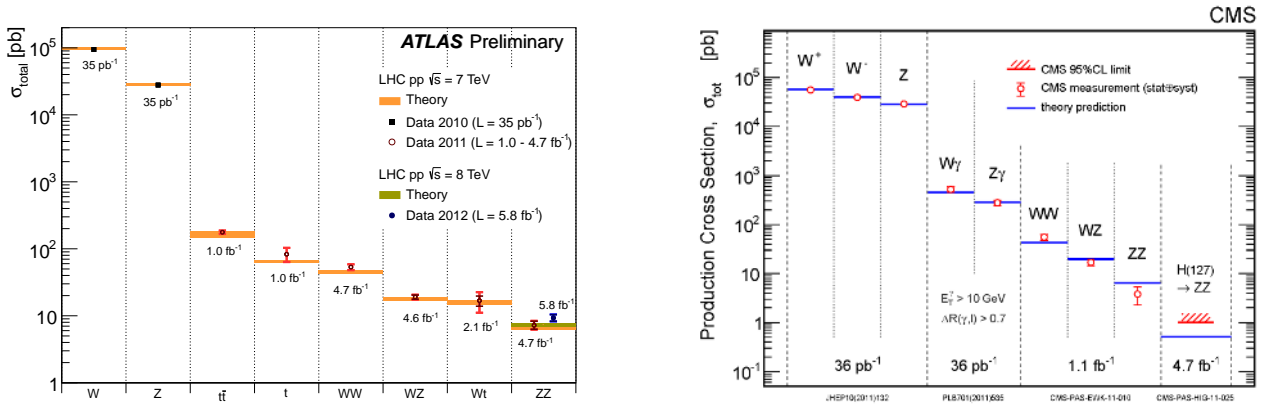


Figure 1. Summary plot for diboson cross-section measurement in ATLAS (left, from public twiki [9]) and CMS (right, from public twiki [10]).

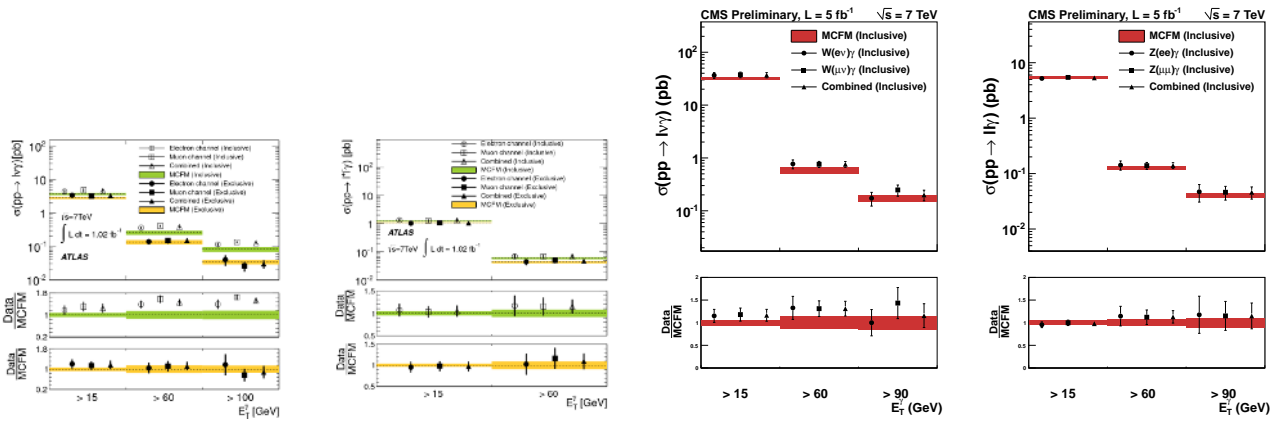


Figure 2. Measured production cross-sections and comparisons to SM NLO predictions for $W + \gamma$ in ATLAS (left), $Z + \gamma$ in ATLAS (middle left, from Figure 3 of [11]), $W + \gamma$ in CMS (middle right) and $Z + \gamma$ in CMS (right, from public twiki [12])

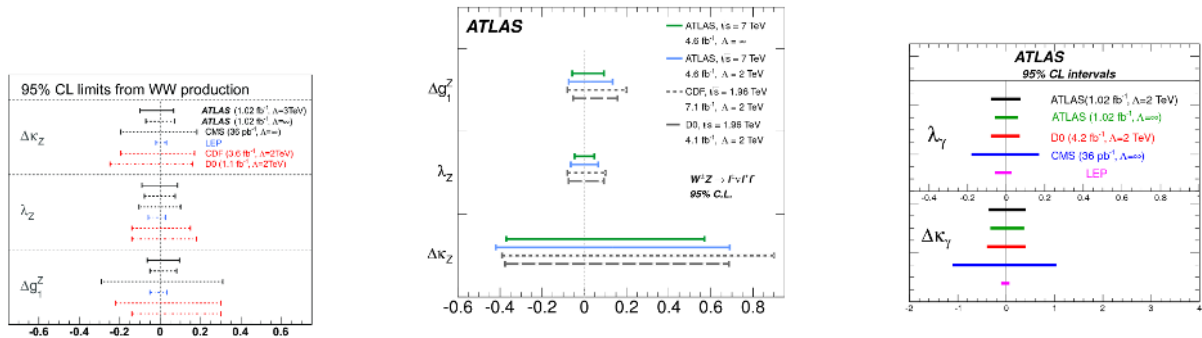


Figure 3. The 95% CI of aTGCs parameters in WWZ and $WW\gamma$ vertices derived from WW (left, from Figure 10 of [13]), WZ (middle, from Figure 5 of [15]) and $W\gamma$ (right, from Figure 4 of [11]) productions.



Figure 4. The 95% CI of aTGCs parameters in ZZ and $ZZ\gamma$ vertices derived from ZZ production in ATLAS (left, from Figure 13 of [19]), CMS (right, from Figure 3 of [20]).

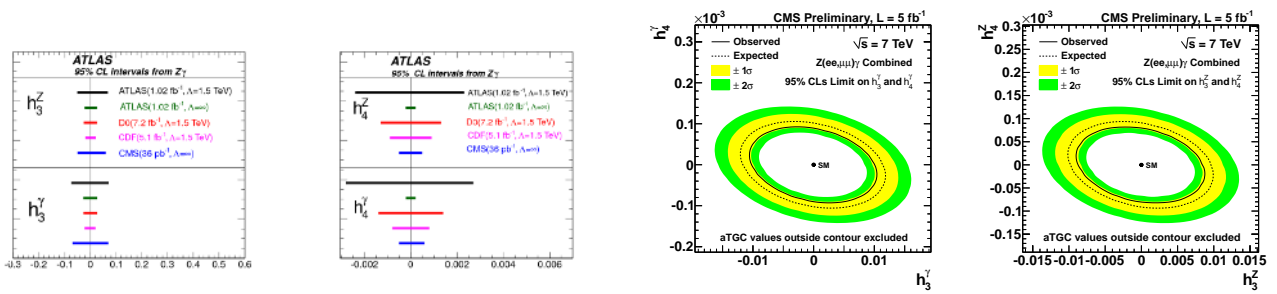


Figure 5. The 95% CI of aTGCs parameters in $ZZ\gamma$ and $Z\gamma\gamma$ vertices derived from $Z\gamma$ production in ATLAS (left two, from Figure 4 of [11]) and CMS (right two, from public twiki [12]).